Experimental 2 Report: X-Rays

Giselle Miralles

March 1, 2024

1 Creation of X-rays with High Energy Electrons

1.1 Direct Measurement

The direct spectrum of X-ray emission was taken using the PHA with the detector placed slightly off-center of the direct beam. The spectrum was taken at 25.00kV and 10.00μA, and the apparatus was set to these conditions for the rest of the experiment. In order to preform a rough energy calibration, the two known x-ray emission peaks of Co-57 were measured. This was done without turning on the x-ray machine and placing the sample in the middle of the apparatus. The calibration data we get from Co-57 is shown in Figure 1.

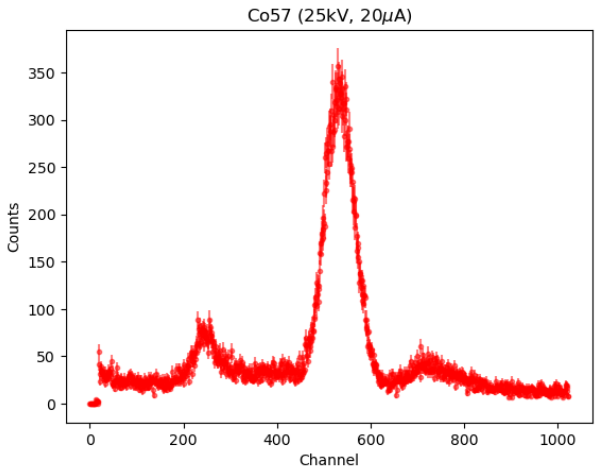

Figure 1: Calibration data from Co-57

To obtain the rough calibration, the location of the energy peaks was estimated by finding local maxima in the PHA software. Using this technique, the x-ray emissions known to have energies 6.4 keV and 14.4 keV were mapped to channels 245 and 531 respectively. The direct energy spectrum was calibrated using the 2-point calibration method in the PHA software. The calibrated spectrum is shown below in Figure 2.

The peak is seen near 8keV and the high energy cutoff is observed at around 16keV.

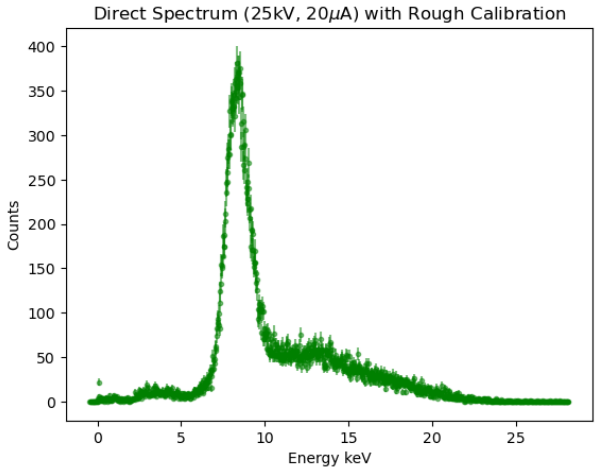

Figure 2: Direct Spectrum with Rough Calibration

1.2 Bragg Scattering

In order to obtain higher resolution and to record the Kα and Kβ peaks, Bragg scattering was used. The setup consisted of placing the LiF crystal in the central post of the apparatus and collecting count measurements under the energy peak at a number of angle increments. Based on our quick scan results, we predicted the Kα and Kβ peaks to be observed at around 40 and 45 degrees. We focused our data collection in these areas, taking smaller increments of angle around this target area. Our angle increments ranged from 1.5 ± 0.1 degrees to 0.5 ± 0.1 degrees. Due to the difficulty associated with attaining a precise angle measurement with the apparatus and the measurement capabilities of the angular reading, a significant window of uncertainty is given to angle measurements.

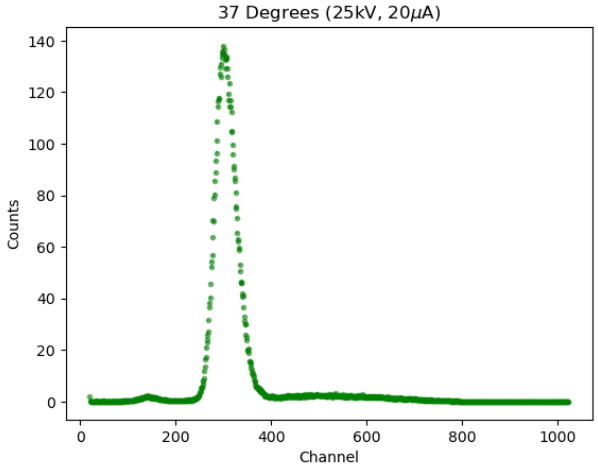

Figure 3: Direct Spectrum with Rough Calibration

A sample spectra taken at 37 degrees is shown below. At every angle measure, we estimated net counts by examining the area under the peak at each angle. Measurements were taken until the net counts under the region of interest equaled approximately 5000 and the collection time was recorded to obtain the final intensity values as rate. Since this peak

shifts slightly at each angle, the region of interest was redefined for each measurement.

The final plot attained from Bragg Scattering is shown in Figure 4. We can see two sharp peaks in intensity at 40 and 44.5 degrees and the high energy cutoff near 13 degrees.

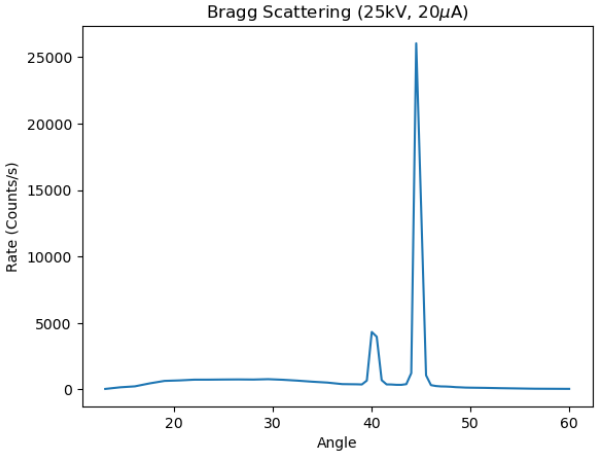

Figure 4: Co-57 Spectrum with Fit

In the peak region, an angle increment of 0.5 degrees was used. Because of the small number of data points in this sharp peak, it is not possible to fit a Gaussian curve to the region in order to determine the exact center point. Instead, the local maxima was found to be at an angle of 40 ± 0.5 and 44.5 ± 0.5 degrees. Uncertainty in maxima is determined by these angle increments used in measurement. There is a high level of uncertainty in the measurements due to the lack of precision in angle measurements.

$$\frac{nhc}{E} = 2d \sin\theta$$

Using the Bragg formula given, and d=0.2008 $\pm$ 0.0001 nm. We can convert these angles to keV. Uncertainty in the energy calculations is propagated using the rules for products and quotients. For the Ka peak at 44.5 degrees, the energy is calculated to be 8.81 ± 0.1 keV. For the Kb peak at 40 degrees, the energy is calculated to be 9.6 ± 0.12 keV. The value n=2 was used to denote the second order since lower values of n are more likely to be detected. These values do not align with out literature values of 8.04 and 8.9 keV respectively. THe uncertainty calculated does not account for various factors in the experiment. Due to the error in final energy value, some systematic errors in angular measurement are most likely at play.

The high energy cutoff in literature is said to be 25kV based on our accelerating voltage. This is near our observed value of the cutoff at 13 degrees or 27 ± 1.04 keV. While it is not in agreement with the literature value, it is closely aligned with what we expect. Since estimating the high energy cutoff is difficult from our plot the estimate of 13 degrees is subject to a high degree of uncertainty.

2 Creation of X-rays by other X-rays

2.1 Calibration

To obtain a proper calibration of energy, a more extensive method of calibration was devised. 3 calibration points were incorporated instead of the previous 2. The first points were attained from the Co-57 spectrum discussed earlier. The third point was taken by removing Zn from the Fluorescence dataset and using the known Kα peak energy to relate it to channel number. Additionally, a more robust method to determine the peak location was used. A Gaussian curve was fit to each of the three energy peaks. Spectra with their Gaussian fits are shown below.

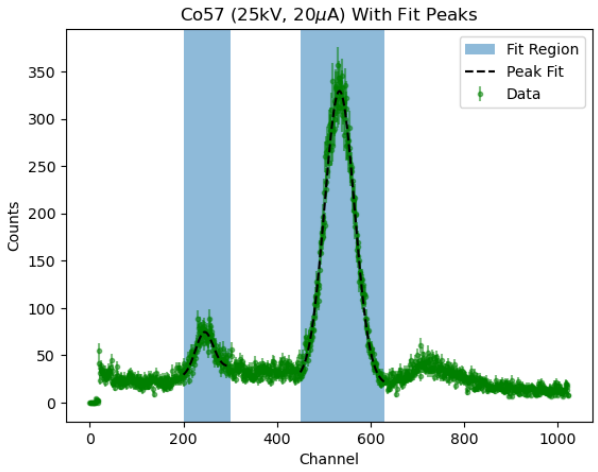

Figure 5: Co-57 Spectrum with Fit

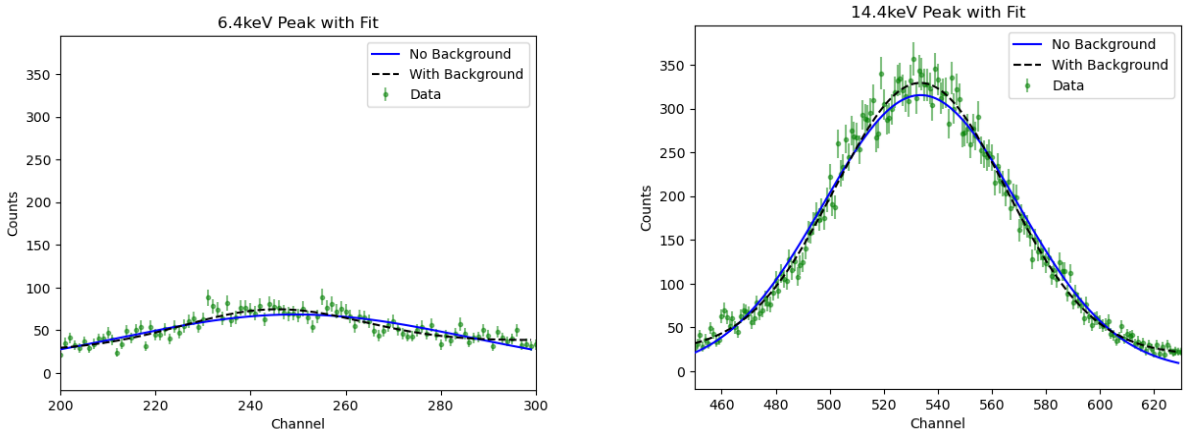

Figure 6: Gaussian Fits of Co-57 Peaks

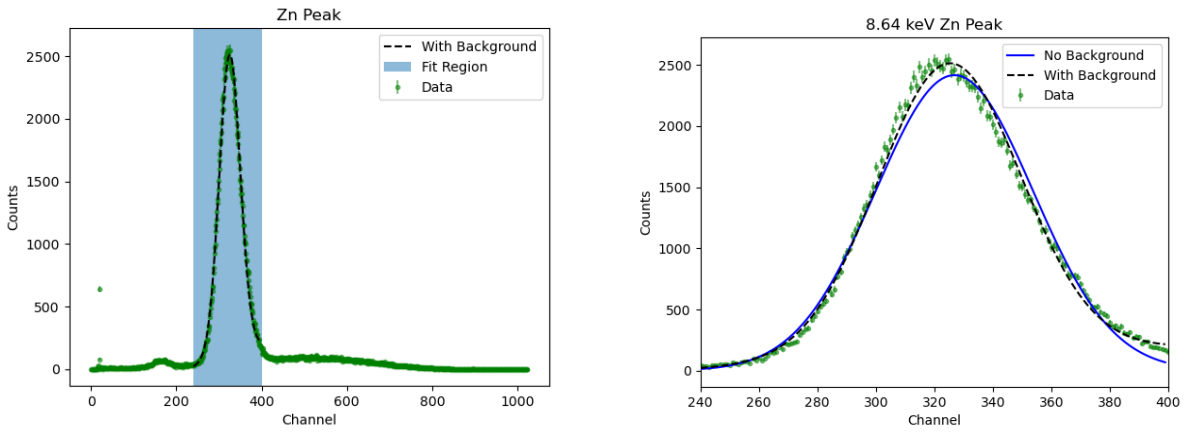

Figure 7: Gaussian Fits of Zn Peak

Using a Gaussian function with a linear background, the parameter μ was extracted to denote the horizontal shift of the curve. The linear background was added to get a more precise fit of the data, which has asymmetrical backgrounds. μ for each of the three peaks with the parameter uncertainty is shown below.

$$f(x) = \frac{N}{\sigma\sqrt{2\pi}} e^{\frac{-(x-\mu)^2}{2\sigma^2}} + mx + b$$

	Energy (keV)	Channel (μ)
Peak 1 (Co-57)	6.4	244.7 ± 1.139e+00
Peak 2 (Co-57)	14.4	533.6 ± 3.070e-01
Zn	8.64	325.1 ± 8.282e-02

Using the three data points attained from this, a linear regression relating channel to energy was preformed on the calibration points (shown in Fig 8). This relation was used to convert channel numbers in the fluorescence data to energy. The uncertainty in the regression fit is also shown in the formula below. This uncertainty was obtained through the parameter uncertainty in the regression.

$$Energy(keV) = \frac{(Channel - (12.36 \pm 0.5002))}{(36.14 \pm 0.05476)}$$

Now that we have a function that can convert channel data to energy, we are able to analyze the fluorescence data.

2.2 Fluorescence and Moseley's Law

The calibrated raw fluorescence spectra are shown for each element in the metal rotary (excluding Zn). For each element, data was collected for 170 seconds. Data for each Kα peak is shown below. A similar method of Gaussian fit was preformed to attain the observed energy for each spectra peak. Each Gaussian fit like before has a parameter μ associated with the horizontal shift of the curve. The uncertainty in the final energy

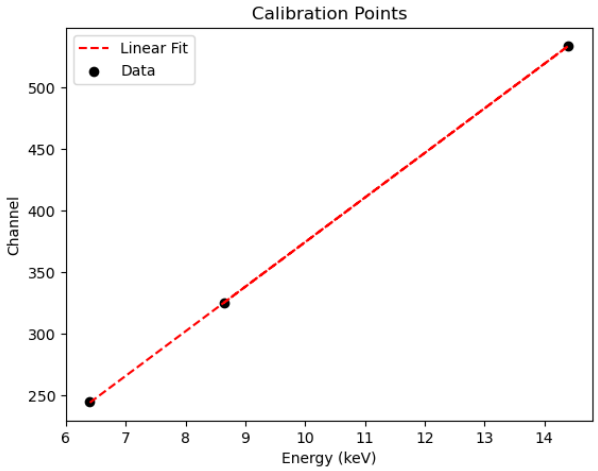

Figure 8: Calibration Regression

is additive of the calibration uncertainty and the parameter uncertainty, following the equation below where α and β are the linear fit parameters in the calibration regression. An estimate of μ with uncertainty in channel units was plugged into the calibration regression to attain an energy estimate. The uncertainty was propagated using standard rules for product and sums. This gives us the final estimates for μ in energy units per metal, which were used for our Moseley's Law comparison.

$$\Delta E = \sqrt{\left(\frac{\Delta c}{b}\right)^2 + \left(\frac{\Delta a}{b}\right)^2 + \left(\frac{(c-a)\cdot \Delta b}{b^2}\right)^2}$$

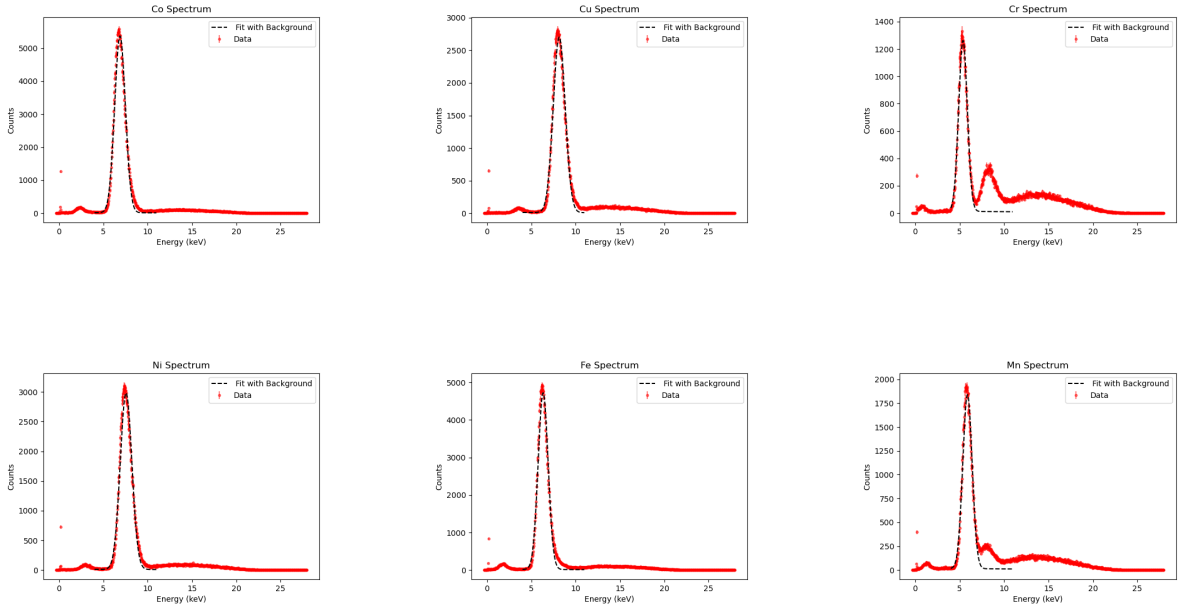

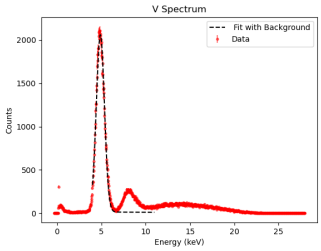

Figure 9: Fluorescence Spectra with Fits

The final data points used in the comparison to Moseley's Law are shown, plotted against Moseley's Law.

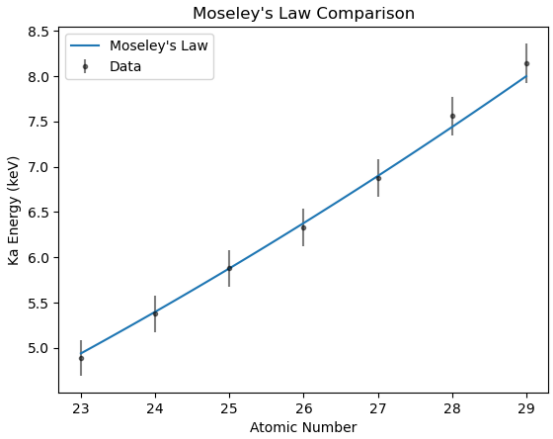

Figure 10: Moseley's Law

The results from comparing Kα energies to Moseley's Law show an agreement with the collected data. Some inconsistencies within the data include the fact that although collection time was held constant, higher count values present in the higher atomic number values might skew the fit parameter inconsistently among the samples. The errors are within the calculated uncertainties of the measured Kα energy. There is a relatively high uncertainty range due to the uncertainty in calibration and peak fit.

2.3 Transmission

The transmission data was collected using a similar technique as the above section on Bragg scattering. From a quick scan, we can observe the range at which the absorption edge is found and make more detailed collections in this region. This region was from 40 to 46 degrees. Observations were taken increments of 0.5 and 1 degrees $\pm$ 0.1, similarly as before. For each angle, data was collected for nickel absorption by placing a nickel sample in the x-ray beam path, and without, to calculate the base rate. Each collection was done for 20 seconds.

Based on the transmission data, we can conclude the transmission edge is between 43.5 and 42.0 degrees. This is the range when the transmission goes from the bottom 10 percentile to the maximum transmission value. When the transmission hits 43 degrees,

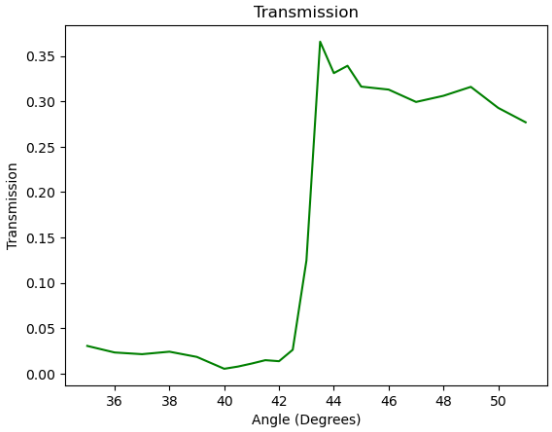

Figure 11: Moseley's Law

transmission jumps 476.9 percent, the largest jump in transmission we experience. Based on the data points collected, we can conclude the transmission edge to be near 43 ± 0.5 degrees. The uncertainty associated with angle is due to the collection increments of the angle measurements. Without extrapolating between data points, we can assume the absorption edge located between within our angle incrimination. Using the Bragg equation from earlier and the second order approximation we find the absorption energy to be 9.02 ± 0.107 keV. Uncertainty in the energy is propagated using the same technique as the earlier section on Bragg scattering.

3 Conclusions and Comparison with Literature

The values for Ka and Kb energies of Copper are shown in the table below. Estimating energy peaks through repeated measurement of rate at varied angles poses many points of potential uncertainty and error that might be minimized if a more direct measurement of energy were to be taken instead. These values yield a significant error compared to the literature values. There are multiple sources of error and uncertainty that could yield the error in our results. There were very limited angle measurements taken in the target ares around the energy peaks. This angle could have yielded a significant error in out final energy calculations. Additionally, the conversion to energy could have been improved with more robust rounding methods.

	Angle	Estimated	Literature
Ka	44.5 ± 0.5	8.81 ± 0.1	8.047
Kb	40 ± 0.5	9.6 ± 0.12	8.904

For the analysis of Moseley's Law, we see an agreement of the data to the law. Looking at a residual plot, we see a slight upward trend signifying higher atomic numbers have a more positive error. While trends in residual plots might signify an improper fit of data, the errors are largely accounted for in the uncertainty values. This would suggest the data is in agreement with Mosley's Law.

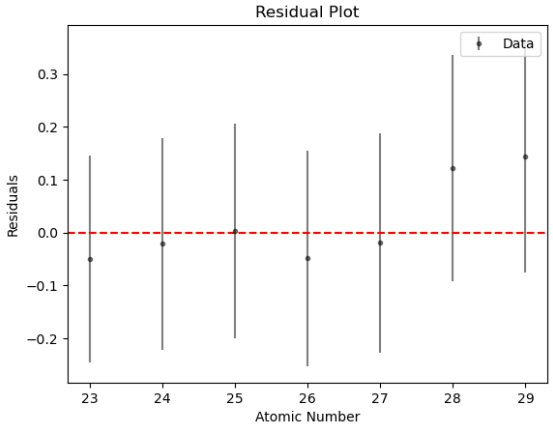

Figure 12: Moseley's Law Residuals

The determination of the Absorption edge also does not agree with literature values. This is likely due to a similar phenomenon in dealing with angle measurement and approximation of the edge. Based on the collected transmission plot, it is difficult to extrapolate the exact numerical angle value that the edge is located at. While we can observe on the plot the sharp increase in transmission, the quantifiable angular point that the edge is said to occur is more difficult to estimate.

	Estimated (keV)	Literature (keV)
Absorption Edge (43 degrees)	9.02 ± 0.107	8.33

Due to the discrepancies in our angular data, it could also be inferred that there could be a bias of the angle measurement on the X-ray apparatus. Over time, the measured angles read on the machine could be further from the true values, and could skew the results that are dependent on angle measurement. While in the estimations of Ka, Kb, and absorption edge, we witness very expected trends, such as the sharp peaks where the Ka and Kb energies are found, we simply see a shifted conversion of those angular values to energies. A similar trend can be seen in the transmission section, where our plot looks as we expected, but attaining the angular measurements and converting to energy yields errors that do not agree with literature.

In the future, I believe another form of verification of our angles would be useful in determining the true incidence angle. It would also be beneficial to take more angle measurements around the angles of 40 and 45 to attain better certainty in angle.